Plant-mediated synthesis of CuO nanoparticles with Allium ampeloprasum extract; application as a glucose non-enzymatic electrochemical sensor

Mobina Eskandari
Qaemshahr Islamic Azad University
Banafsheh Norouzi (norouz2020@yahoo.com)
Qaemshahr Islamic Azad University

Short Report

Keywords: CuO nanoparticles, Allium ampeloprasum, Extract, Glucose, Non_enzymatic sensor

Posted Date: June 22nd, 2022

DOI: https://doi.org/10.21203/rs.3.rs-1761661/v1

Abstract

A simple synthesis using *Allium ampeloprasum* plant extract as a reducing agent has been done for the preparation of CuO nanoparticles (CuO NPs). Firstly, copper ions are reduced to copper atoms by plant extract, and then, they could be changed to CuO during calcination. Some techniques such as X-ray diffraction (XRD), UV-Visible (UV-Vis), Fourier-transform infrared (FT-IR), scanning electron microscopy (SEM), and electrochemical methods have been applied to the evaluation of the CuO NPs formation. A modified carbon paste electrode with CuO (CPE/CuO) was prepared and employed for the non-enzymatic amperometric sensor of glucose. The linear dynamic range of this modified electrode and the limit of detection (LOD) were 1-120 μmol L^{-1} and 0.8 μmol L^{-1} (3δ), respectively. Simplicity, low cost, and easily of preparation are the prominent features of this sensor. Also, the stability, reproducibility, and repeatability of this modified electrode are acceptable.

1. Introduction

Allium ampeloprasum is a member of the onion genus *Allium.* The wild plant is commonly known as wild leek or broadleaf wild leek. This plant is native to regions from southern Europe to western Asia, but it is cultivated in many other places and has become naturalized in many countries. The ethanolic extract of *Allium ampeloprasum* is a good source of alkaloids, steroids, terpenoids, flavonoids, tannins, saponins, reducing sugars, proteins, and oil. These results suggested it can be used as a natural antioxidant [1].

The copper-oxygen system has two stable stoichiometric oxides, cuprous oxide (Cu_2O) and cupric oxide (CuO). They have cubic and monoclinic crystal structures with a direct bandgap in the range of 2.0–2.5 eV and 1.3–1.7 eV, respectively [2].

CuO NPs have many applications in various fields of science such as gas sensors [3–7], catalysts [8–10], superconductors [11], and magnetic phase transition [12]. So far, various methods have been reported for the preparation of CuO NPs such as sonochemical synthesis [13, 14], ultrasonic spray pyrolysis [15], hydrothermal synthesis [16], solid-state reaction method [17], the electrochemical method [18], and solution-based methods such as sol-gel synthesis [19], and precipitation-pyrolysis [20]. Green synthesis is a procedure for the preparation of NPs. It was proceeded via plant material, agricultural waste, or enzymes. This method is uncomplicated, low-cost, and has less usage of perilous chemicals [21, 22]. It can be an environmental friendliness route. There are some reports about the green synthesis of CuO NPs by *Calotropis gigantea* leaves extract [23], *Chamomile* flower extract [24], the leaf extract of *Bauhinia tomentosa* [25], *Enicostemma axillare (Lam.)* leaf extract [26], *Lantana camara* flower extract [27], etc.

The monitoring of glucose is very important because of clinical and industrial points of view [28]. The fabrication of glucose enzyme electrodes is one of the procedures to determine glucose. Glucose oxidase (Gox) is used in the structure of these electrodes as an enzyme. There are some disadvantages of enzymes such as high cost, instability, and complicated procedure for immobilization [29]. Also, the catalytic activity of Gox is easily affected by temperature, pH value, humidity, ionic detergents, and toxic

chemicals [29]. Therefore, many efforts have been done by non-enzymatic sensors with metal nanoparticles such as gold [30], Pt [31], Ag [32], Ni [33], Cu [34], and metal oxide nanoparticles such as NiO [35, 36], ZnO [37], and CuO [38–40] for the determination of glucose. However, the development of a low-cost, simple and effective sensor for the detection of enzyme-free glucose is still greatly demanded.

In our previous works, we fabricated a non-enzymatic sensor for the determination of glucose by CPE/poly (isonicotinic acid) (SDS) Ni-Co [41]. We also reported the green synthesis of some NPs such as Co_3O_4 NPs [42], Pt NPs [43], CdO NPs [44, 45], and NiO NPs [46] by plant extract.

In this paper, we first described a simple and low cost procedure for the preparation of

CuO NPs by *Allium ampeloprasum* plant extract with the size of about 24 nm. Then, CPE/CuO NPs have been fabricated as a non-enzymatic sensor for the determination of glucose.

2. Material And Methods

2.1. Reagents and materials

Copper chloride, glucose, ethanol, and sodium hydroxide were purchased from Merck (New Jersey, US) origin. Graphite powder (particle diameter 0.10 mm) from Merck (New Jersey, US) and high viscosity paraffin (density 0.88 g cm^{-3}) from Fluka (Sydney, Australia) were used as the substrate and the pasting liquid for the preparation of CPE. Deionized water (DW) was used in the preparation of all aqueous solutions.

2.2. Apparatus

The identification of phase, purity, and crystallite size was determined by XRD (X'Pert PRO diffractometer system, Panalytical company, United Kingdom) using Cu K_α radiation with (λ = 1.5418 Å) in the range of $2\theta = 20–80^\circ$ at room temperature. The characterization of morphology has been performed by SEM (Zeiss Sigma VP, Germany).

A potentiostat/galvanostat μ-Autolab type III modular system (Eco Chemie BV, the Netherlands) was used for electrochemical experiments. It has been equipped with electrochemical software (Nova). A CPE/CuO NPs was employed as a working electrode, an Ag|AgCl|KCl (3 M) as the reference electrode, and a platinum wire as a counter electrode. Amperometric measurements were carried out at 0.1 V under a magnetically stirred condition. All experiments were carried out at room temperature (25 ℃). Deaeration has been done by importing nitrogen gas into the solution.

2.3. Preparation of CuO NPs

First, *Allium ampeloprasum* plant was thoroughly washed with DW and this plant was dried at room temperature and in shade. About, 60 g of it was transferred to a 1000 mL beaker containing 500 mL

ethanol. Then, it was kept for five overnights. Finally, the ethanolic extract was obtained via filtration using Whatman filter paper and it was used as the extract for the synthesis of CuO NPs.

The preparation of CuO NPs has been done by a hydrolysis process using aqueous copper chloride (250 mL, 0.1 M) as a precursor and NaOH (The concentrated NaOH solution was added dropwise to raise the pH of the reaction mixture to 10 where a large amount of the precipitate was produced) as the hydrolyzing agent in the presence of plant extract of *Allium ampeloprasum* (250 mL, 120 g L^{-1}) under continuous stirring for 2 h. The solution was kept overnight and then centrifuged. Finally, the solid mass was calcined in a furnace at 400°C for 2 h to remove the hydroxyl ions or water molecules if any attached to the product, which resulted in a black-red solid mass (Fig. 1). Phenolic compounds and flavonoids in plant extract are as a reducing agents and reduced copper ions to copper. Then, they changed to copper oxide during calcination. It was analyzed by some techniques.

2.4. Preparation of CPE/CuO

preparation of CPE/CuO NPs has been done by mixing CuO NPs (10% w/w) and graphite

powder in the presence of a suitable amount of liquid paraffin (25 % w/w). Then, this mixture was blended by hand mixing with a mortar and pestle for 20 min until a uniformly wetted paste was obtained. The resulting paste was then inserted into the bottom of a glass tube (internal

radius 1.7 mm). The electrical connection was via a copper wire lead fitted to the glass tube. A fresh electrode surface was generated rapidly by extruding a small plug of the paste and smoothing the resulting surface on white paper until a smooth shiny surface was observed.

3. Results And Discussion

3.1. Characterization of CuO

XRD technique has been used to characterize the crystallization structure and

average size of synthesized CuO NPs. Figure 2 shows XRD patterns synthesized by $CuCl_2$ and *Allium ampeloprasum* extract. Diffraction peaks assigned to CuO at $2\theta = 35^\circ$, 40°, 47°, 54°, 57°, 60° and 65° corresponding to the planes (002), (111), (202), (020), (202), (113) and (311) respectively of monoclinic phase CuO (JCPDS file no.: 48-1548) [47].

Based on the highest peak in the XRD spectra ($2\theta = 40^\circ$), the average crystallite size of NPs has been estimated to be 24.6 nm using the Debye-Scherrer formula. It is equal to $D = K\lambda/ß\cos\theta$, where D is crystallite size, K is the Scherer constant usually taken as 0.89, λ is 0.15418 nm for CuK_α, and ß is full-width half maximum of diffraction peak measured at 2θ [48].

Figure 3 depicts the UV–Vis absorption spectra of CuO NP synthesized of *Allium ampeloprasum* extract. It shows a peak at 247 nm which is in close agreement with the earlier reports [49, 50].

FT-IR spectra for the synthesized CuO NPs are given in Fig. 4. The strong peaks observed at 3444, 1622, 1385 and 987 cm^{-1} corresponds to stretching vibrations of O-H, C = C, aliphatic C–H, and C–O, respectively. The peaks at 477, 515, and 596 cm^{-1} correspond to CuO vibration of CuO NPs [50]. These results confirm the presence of a thin layer of plant chemical compounds on the NPs.

The morphology of CuO NPs was investigated by SEM method. Figure 5 shows SEM images of CuO NP synthesized of *Allium ampeloprasum* extract. These images show almost uniform structures with nanometer particle size. Figure 5c shows the particle size distribution curve of CuO NPs. Based on these results the mean size of the particles is about 41.43 nm. This result is almost consistent with the XRD results.

3.2. Electrochemical behavior of CPE/CuO NPs

Figure 6 shows Cyclic voltammograms of CPE/CuO NPs during six consecutive potential sweeps in 0.1 mol L^{-1} NaOH solution in the potential range of – 1.0 to 1.0 V with a scan rate of 50 mV s^{-1}. It is done to activate copper sites on the electrode surface. The appearance of the anodic and cathodic peaks of the Cu (III)/Cu (II) redox pair indicates the presence of copper signal on the electrode surface. Based on the results, the reaction can be considered as follows:

$$CuO + OH^- \longleftrightarrow CuOOH + e^- \qquad (1)$$

Figure 7 shows the cyclic voltammograms of CPE and CPE/CuO NPs in solution containing potassium ferrocyanide in the potential range of -0.2 to 1.0 V. According to this figure, the current response at the surface of the CPE/CuO NPs is higher than that of the CPE. Experimental results show that the cathodic and anodic peaks in Fig. 7 are related to the redox pair $Fe(CN)_6^{3-}/Fe(CN)_6^{4-}$. The difference between anodic and cathodic currents on the surface of CPE and CPE/CuO NPs indicates a larger electroactive surface in the CPE/CuO NPs compared to CPE.

The active surface areas of the modified electrode are calculated by the cyclic voltammetry technique. The Randles–Sevcik formula can be used at various scan rates using $K_4Fe(CN)_6$ solution as following [51]:

$$I_{pa} = 0.4463AC_0(F^3/RT)^{1/2}n^{3/2}D_R^{1/2}v^{1/2} \qquad (2)$$

Where I_{pa}, A, C_0, F, R, T, n, D, v, A is anodic peak current (A), active surface area of the electrode (cm^2), concentration of ferrocyanide (mol cm^{-3}), Faraday constant (96500 C mol^{-1}), gas constant (8.314 J mol^{-1} K^{-1}), the absolute temperature (298 ^{0}K), the number of electrons, diffusion constant (cm^2 s^{-1}), and the potential scan rate (V s^{-1}), respectively. The value of D is 7.16×10^{-6} cm^2 s^{-1} for 1 mmol L^{-1} ferrocyanide in 0.1 mol L^{-1} potassium chloride. The slope I_{pa} versus $v^{1/2}$ was 1.8×10^{-5} A $(V\ s^{-1})^{1/2}$. Therefore, the active microscopic surface area was found to be 0.024 cm^2 for CPE/CuO NPs compared with 0.016 cm^2 for CPE. The geometric surface of the two electrodes is exactly the same. Therefore, these results confirm the presence of CuO NPs increases the active surface area of the modified electrode.

Figure 8 shows the cyclic voltammetric responses of CPE and CPE/CuO NPs in the wide potential range at a scan rate of 20 mV s^{-1} in 0.1 mol L^{-1} NaOH solution. As shown in this figure, there is no obvious peaks on the CPE but it is an obvious anodic peak for CPE/CuO NPs in the presence of 10 µmol L^{-1} glucose. Also, the current response was increased when the concentration of glucose in the NaOH solution was increased (Fig. 8C). These observations confirm the electrocatalytic effect of CuO in the presence of glucose. The electrocatalytic oxidation of glucose on CuO NPs by Cu(II)/Cu(III) redox couple in 0.1 mol L^{-1} NaOH is generally expressed as following reaction:

$$\mathrm{CuOOH + Glucose \longrightarrow Cu(OH)_2 + products} \qquad (3)$$

First, Cu (II) species is oxidized to Cu (III) at the surface of CPE/CuO NPs in 0.1 mol L^{-1} NaOH. Then, Cu (III) species can be converted to Cu (II) by chemical reaction with glucose (electrocatalytic oxidation or EC'). In the presence of glucose, it helps to progress the first step of the reaction (further production of CuOOH or Cu (III)).

According to previous studies, carbohydrates are oxidized at high pH levels [41]. Also, the formation of CuOOH has been done in alkaline solution. However, in this work, the oxidation of glucose was studied at the surface of CPE/CuO NPs in 0.1 mol L^{-1} NaOH.

Amperometry technique was used to find the limit of detection (LOD), and Linear dynamic range (LDR) of CPE/CuO NPs in the presence of glucose in 0.1 mol L^{-1} NaOH solution. Figure 9A depicts amperogram of CPE/CuO NPs with the addition of glucose into a stirred 0.1 mol L^{-1} NaOH at an applied potential of 0.1 V every 30 second. Figure 9B shows the calibration curve for the CPE/CuO NPs in the presence of different concentrations of glucose. The linear response has been seen at the concentration range of 1–120 µmol L^{-1}. LOD was 0.8 µmol L^{-1} when the signal to noise ratio was 3 (S/N = 3).

The Tafel plot (Log I vs. E) is investigated for CPE/CuO NPs in the presence of 1 mmol L^{-1} glucose (not shown). The Tafel slope is equal to n (1-α) F/2.303RT, where n is the number of electrons involved in the rate determining step, α is the transfer coefficient, F is the Faraday constant (96500 C mol^{-1}), R is the

molar gas constant (8.314 J K^{-1} mol^{-1}), and T is temperature (298 ^{0}K). Considering one electron transfer to be the rate-limiting step, the α value was equal to 0.65.

3.3. Interferences studies

Amperometric method was used to study interferences. Amperometric responses of CPE / CuO NPs was performed in 0.1 mmol L^{-1} glucose at an applied potential of 0.1 V in 0.1 mol L^{-1} NaOH solution and in the presence of uric acid (UA) and ascorbic acid (AA) with the same concentration (Fig. 10). The current responses did not change with addition of UA and AA. These results were shown that these species do not interfere with glucose measurement.

3.4. The electrode stability, repeatability, and reproducibility

Stability for the CPE/CuO NPs was examined by cyclic voltammetry method with recording its 40 consecutive curves in 0.1 mol L^{-1} NaOH solution at a scan rate of 50 mV s^{-1}.

The slight changes have been observed in the peak current (< 5%). Cyclic voltammograms of four CPE/CuO NPs were investigated in 0.1 M NaOH in the presence of 10 µmol L^{-1} glucose. The relative standard deviation (RSD) for the electrocatalytic oxidation currents was estimated about 4.3 %. It was indicated a high reproducibility. Also, five parallel determination has been done by a CPE/CuO NPs in the presence of 10 µmol L^{-1} of glucose with RSD of 3.5 %. It confirms the high repeatability.

4. Conclusion

In this study, biosynthesis of CuO NPs has been done using *Allium ampeloprasum* extract and copper chloride that it is a simple and low-cost method. The CuO NPs were characterized by different methods such as UV-Vis (λ_{max} = 247 nm), XRD (crystallite size = 24.6 nm) and SEM (particle size = 41.4 nm). The CPE/CuO NPs can be used as a suitable and low-cost electrocatalyst for the oxidation of glucose. LDR and LOD values were 1–120 µmol L^{-1} and 0.8 µmol L^{-1}, respectively. The main advantage of this electrode compared with other electrodes in Table 1 is greater shift in over-potential (anodic peak potential = 0.05 V).

Table 1

Comparison of the performance of the proposed CPE/CuO with other modified electrodes.

Electrode	pH	Applied potential, V vs Ag | AgCl | KCl (3 mol L^{-1})	LDR, μmol L^{-1}	LOD, μmol L^{-1}	Reference
SPE[a]/CuO	13	0.6	50–600	4	[52]
CPE/PINA[b] (SDS)/$Ni_{80}Co_{20}(OH)_2$	13	0.5	10–370	8.3	[41]
GCE/Nf[c]/ CuO NPs	13	0.6	40–6000	5	[53]
GCE/Nf/CuO NPlts[d]	13	0.5	50–600	0.25	[54]
CPE/CuO NPs	13	0.05	1–120	0.8	Present work

[a]Screen printed electrode

[b]Poly (isonicotinic acid)

[c]Nafion

[d]Platelet

Declarations

Acknowledgment

The authors wish to thanks Islamic Azad University in Qaemshahr Branch for the institutional support.

Conflict of interest

The authors declare no competing interest

References

1. F.A.E.R.A.A. El-Rehem, R.F.M. Ali, Proximate compositions, phytochemical constituents, antioxidant activities and phenolic contents of seed and leaves extracts of Egyptian leek (Allium ampeloprasum var. kurrat), Eur. J. Chem. 4 (2013) 185-190.
2. D. Gupta, S.R. Meher, N. Illyaskutty, Z.C. Alex, Facile synthesis of Cu_2O and CuO nanoparticles and study of their structural, optical and electronic properties, J. Alloys Compd. 743 (2018) 737–745.
3. D. Li, Y. Tang, D. Ao, X. Xiang, S. Wang, X. Zu, Ultra-highly sensitive and selective H_2S gas sensor based on CuO with sub-ppb detection limit, Int. J. Hydrog. Energy 44 (2019) 3985-3992.
4. U.T. Nakate, G.H. Lee, R. Ahmad, P. Patil, Y.B. Hahn, Y.T. Yu, E.K. Suh, Nano- bitter gourd like structured CuO for enhanced hydrogen gas sensor application, Int. J. Hydrog. Energy 43 (2018) 22705-22714.
5. [5] F. Wang, H. Li, Z. Yuan, Y. Sun, F. Chang, H. Deng, L. Xie, H. Li, A highly sensitive gas sensor based on CuO nanoparticles synthetized *via* a sol–gel method, RSC. Adv. 83 (2016) 79343-79349.
6. S. Steinhaur, E. Brunet, T. Maier, G.C. Mutinati, A. Kock, O. Freundenberg, C. Gspan, W. Grogger, A. Neuhold, R. Resel, Gas sensing properties of novel CuO nanowire Devices, Sens. Actuators B Chem. 187 (2013) 50-57.
7. A. Bejaoui, J. Guerin, J.A. Zapien, K. Aguir, Theoretical and experimental study of the response of CuO gas sensor under ozone, Sens. Actuators B Chem. 190 (2014) 8-15.
8. S. Sukumar, A. Rudrasenan, D.P. Nambiar, Green-synthesized rice-shaped copper oxide nanoparticles using *Caesalpinia bonducella* seed extract and their applications, ACS Omega 5 (2020) 1040-1051.
9. M. Nasrollahzadeh, M. Maham, S.M. Sajadi, Green synthesis of CuO nanoparticles by aqueous extract of *Gundelia tournefortii* and evaluation of their catalytic activity for the synthesis of *N*-monosubstituted ureas and reduction of 4-nitrophenol, J. Colloid Interface Sci. 455 (2015) 245-253.
10. M. Mirabedini, E. Motamedi, M.Z. Kassaee, Magnetic CuO nanoparticles supported on graphene oxide as an efficient catalyst for A^3-coupling synthesis of propargylamines, Chin. Chem. Lett. 26 (2015) 1085-1090.
11. A.K. Mishra, A.K. Nayak, A.K. Das, D. Pradhan, Microwave-assisted solvothermal synthesis of cupric oxide nanostructures for high-performance supercapacitor, J. Phys. Chem. C 122 (2018) 11249–11261.
12. J.M. Wesselinowa, Magnetic properties of doped and undoped CuO nanoparticles taking into account spin–phonon interactions, Phys. Lett. A 375 (2011) 1417-1420.
13. G. Bhanjana, N. Dilbaghi, K.H. Kim, S. Kumar, Low temperature synthesis of copper oxide nanoflowers for lead removal using sonochemical route, J. Mol. Liq. 244 (2017) 506-511.
14. S. Anandan, G.J. Lee, J.J. Wu, Sonochemical synthesis of CuO nanostructures with different morphology, Ultrason. Sonochem. 19 (2012) 682-686.

15. I. Singh, G. Kaur, R.K Bedi, CTAB assisted growth and characterization of nanocrystalline CuO films by ultrasonic spray pyrolysis technique, Appl. Sur. Sci. 257 (2011) 9546–9554.
16. [16] H. Siddiqui, M.S. Qureshi, F.Z. Haque, One-step template-free hydrothermal synthesis of CuO tetrapods, Optik 125 (2014) 4663–4667.
17. S. Sohrabnezhad, A. Valipour, Synthesis of Cu/CuO nanoparticles in mesoporous material by solid state reaction, Spectrochim. Acta A Mol. Biomol. Spectrosc. 114 (2013) 298–302.
18. R. Katwal, H. Kaur, G. Sharma, M. Naushad, D. Pathania, Electrochemical synthesized copper oxide nanoparticles for enhanced photocatalytic and antimicrobial activity, J. Ind. Eng. Chem. 31 (2015) 173–184.
19. Z.N. Kayani, M. Umer, S. Riaz, S. Naseem, Characterization of Copper Oxide Nanoparticles Fabricated by the Sol–Gel Method, J. Electron. Mater. 44 (2015) 3704–3709.
20. [20] H. Fan, L. Yang, W. Hua, S. Xie, Controlled synthesis of monodispersed CuO Nanocrystals, Nanotechnol. 15 (2004) 37-51.
21. T.B. Vidovix, H.B. Quesada, E.F.D. Januario, R. Bergamasco, A.M.S. Vieira, Green synthesis of copper oxide nanoparticles using Punica granatum leaf extract applied to the removal of methylene blue, Mater. Lett. 257 (2019) 126685.
22. G. Sharmila, M. Thirumarimurugan, C. Muthukumaran, Green synthesis of ZnO nanoparticles using Tecoma castanifolia leaf extract: characterization and evaluation of its antioxidant, bactericidal and anticancer activities, Microchem. J. 145 (2019) 578–587.
23. J.K. Sharma, M.S. Aktar, S. Ameen, P. Srivastava, Singh, G. Green synthesis of CuO nanoparticles with leaf extract of *Calotropis gigantea* and its dye-sensitized solar cells applications, J. Alloy Compd. 632 (2015) 321–325.
24. F. Duman, I. Ocsoy, F.O. Kup, Chamomile flower extract-directed CuO nanoparticle formation for its antioxidant and DNA cleavage properties, Mater. Sci. Eng. 60 (2016) 333–338.
25. G. Sharmila, R. Pradeep, K. Sandiya, S. Santhiya, C. Muthukumaran, J. Jeyanthi, N.M. Kumar, M. Thirumarimurugan, Biogenic synthesis of CuO nanoparticles using *Bauhinia tomentosa* leaves extract: Characterization and its antibacterial application, J. Mol. Struct. 1165 (2018) 288–292.
26. S.C. Mali, S. Raj, R. Trivedi, Biosynthesis of copper oxide nanoparticles using *Enicostemma axillare (Lam.)* leaf extract, Biochem. Biophys. Rep. 20 (2019) 100699.
27. R. Chowdhury, A. Khan, M.H. Rashid, Green synthesis of CuO nanoparticles using *Lantana camara* flower extract and their potential catalytic activity towards the aza- Michael reaction, Rsc. Adv. 10 (2020) 14374–14385.
28. J. Luo, S. Jiang, H. Zhang, J. Jiang, X. Liu, A novel non-enzymatic glucose sensor based on Cu nanoparticle modified graphene sheets electrode, Anal. Chim. Acta 709 (2012) 47–53.
29. S. Bilal, W. Ullah, A.U.H.A. Shah, Polyaniline@CuNi nanocomposite: A highly selective, stable and efficient electrode material for binder free non-enzymatic glucose sensor, Electrochim. Acta 284 (2018) 382–391.

30. D. Feng, F. Wang, Z. Chen, Electrochemical glucose sensor based on one-step construction of gold nanoparticle–chitosan composite film, Sens. Actuators B Chem. 138 (2009) 539–544.
31. L.T. Hoa, K.G. Sun, S.H. Hur, Highly sensitive non-enzymatic glucose sensor based on Pt nanoparticle decorated graphene oxide hydrogel, Sens. Actuators B Chem. 210 (2015) 618–623.
32. M. Baghayeri, A. Amiri, S. Farhadi, Development of non-enzymatic glucose sensor based on efficient loading Ag nanoparticles on functionalized carbon nanotubes, Sens. Actuators B Chem. 225 (2016) 354–362.
33. H. Jia, N. Shang, Y. Feng, H. Ye, J. Zhao, H. Wang, C. Wang, Y. Zhang, Facile preparation of Ni nanoparticle embedded on mesoporous carbon nanorods for non- enzymatic glucose detection, J. Colloid Interface Sci. 583 (2021) 310–320.
34. J. Jiang, P. Zhang, Y. Liu, H. Luo, A novel non-enzymatic glucose sensor based on a Cu-nanoparticle-modified graphene edge nanoelectrode, Anal. Methods 9 (2017) 2250–2210.
35. S. Liu, B. Yu, T. Zhang, A novel non-enzymatic glucose sensor based on NiO hollow Spheres, Electrochim. Acta 102 (2013) 104–107.
36. H. Zhang, S. Liu, Nanoparticles-assembled NiO nanosheets templated by graphene oxide film for highly sensitive non-enzymatic glucose sensing, Sens. Actuators B Chem. 238 (2017) 788–794.
37. T. Dayakar, K. Venkateswara, K. Rao, K. Bikshalu, V. Rajendar, P. Si-Hyun, Novel synthesis and structural analysis of zinc oxide nanoparticles for the non-enzymatic glucose biosensor, Mater. Sci. Eng. 75 (2017) 1472–1479.
38. F. Huang, Y. Zhang, J. Chen, S. Li, Y. Li, F. Wang, S. Feng, Nonenzymatic glucose sensor based on three different CuO nanomaterials, **Anal. Methods 5** (2013) 3050-3055.
39. Y. Tian, Y. Liu, W.P. Wang, X. Zhang, W. Peng, CuO nanoparticles on sulfur-doped graphene for nonenzymatic glucose sensing, Electrochim. Acta 156 (2015) 244–251.
40. A. Ashok, A. Kumar, F. Tarlochan, Highly efficient nonenzymatic glucose sensors based on CuO nanoparticles, Appl. Surf. Sci. 481 (2019) 712–722.
41. R. Ojani, J.B. Raoof, B. Norouzi, Performance of glucose electrooxidation on Ni–Co composition dispersed on the poly (isonicotinic acid) (SDS) film, J. Solid State Electrochem. 15 (2011) 1139–1147.
42. M. Fallahi, B. Norouzi, Synthesis of cobalt oxide nanoparticles using Cirsium vulgare leaves extract and evaluation of electrocatalytic effects on oxidation of L-cysteine, Ionics 26 (2020) 1951–1961.
43. A.R. Mohamadi, N. Nami, B. Norouzi, Bio-directed synthesis of platinum nanoparticles by Nymphaea alba extract: fabrication of a novel nonenzymatic hydrogen peroxide sensor, J. Mater Sci: Mater. Electron. 31 (2020) 18721–18731.
44. S. Kaveh, B. Norouzi, N. Nami, A. Mirabi, Phytochemical synthesis of CdO nanoparticles: fabrication of electrochemical sensor for quantification of cefixime, J. Mater. Sci. Mater. Electron, 32 (2021) 8932–8943.

45. S. Kaveh, N. Nami, B. Norouzi, A. Mirabi, Biosynthesis of (MWCNTs)-COOH/CdO hybrid as an effective catalyst in the synthesis of pyrimidine-thione derivatives by water lily flower extract, Inorg. Nano-Met. Chem. 51 (2021) 1459–1470.
46. S. Abbasnejad, B. Norouzi, Biosynthesis of nano nickel oxide powder using Malva sylvestris; evaluation of electrocatalytic activity for determination of cephalexin in real samples, Russ. J. Electrochem. 57 (2021) 478–489.
47. L. Dorner, C. Cancellieri, B. Rheingans, M. Walter, R. Kagi, P. Schumtz, M.V. Kovalenko, L.P.H. Jeurgens, Cost-effective sol-gel synthesis of porous CuO nanoparticle aggregates with tunable specific surface area, Sci. Rep. 9 (2019) 11758.
48. H.P. Klug, L.E. Alexander, X-ray Diffraction Procedures, 2nd edn, Wiley, New York, 1964.
49. R. Sivaraj, P.K.S.M. Rahman, P. Rajiv, S. Narendhran, R. Venckatesh, Biosynthesis and characterization of *Acalypha indica* mediated copper oxide nanoparticles and evaluation of its antimicrobial and anticancer activity, Spectrochim. Acta, Part A 129 (2014) 255–258.
50. D. Renuga, J. Jeyasundari, A.S.S. Athithan, Y.B.A. Jacob, Synthesis and characterization of copper oxide nanoparticles using *Brassica oleracea var. italic* extract for its antifungal application, Mater. Res. Express 7 (2020) 045007.
51. A.J. Bard, L.R. Faulkner, Electrochemical Methods: Fundamentals and Applications, Wiley, New York, 2001.
52. N.A. Choudhry, D.K. Kampouris, R.O. Kadara, N. Jenkinso, C.E. Banks, Next generation screen printed electrochemical platforms: Non-enzymatic sensing of carbohydrates using copper(II) oxide screen printed electrodes, Anal. Methods 1 (2009) 183–187.
53. F. Huang, Y. Zhong, J. Chen, S. Li, Y. Li, F. Wang, S. Feng, Nonenzymatic glucose sensor based on three different CuO nanomaterials, Anal. Methods 5 (2013) 3050–3055.
54. S. Felix, P. Kollu, B.P.C. Raghupathy, S.K. Jeong, A.N. Grace, Electrocatalytic oxidation of carbohydrates and dopamine in alkaline and neutral medium using CuO nanoplatelets, J. Electroanal. Chem. 739 (2015) 1–9.

Figures

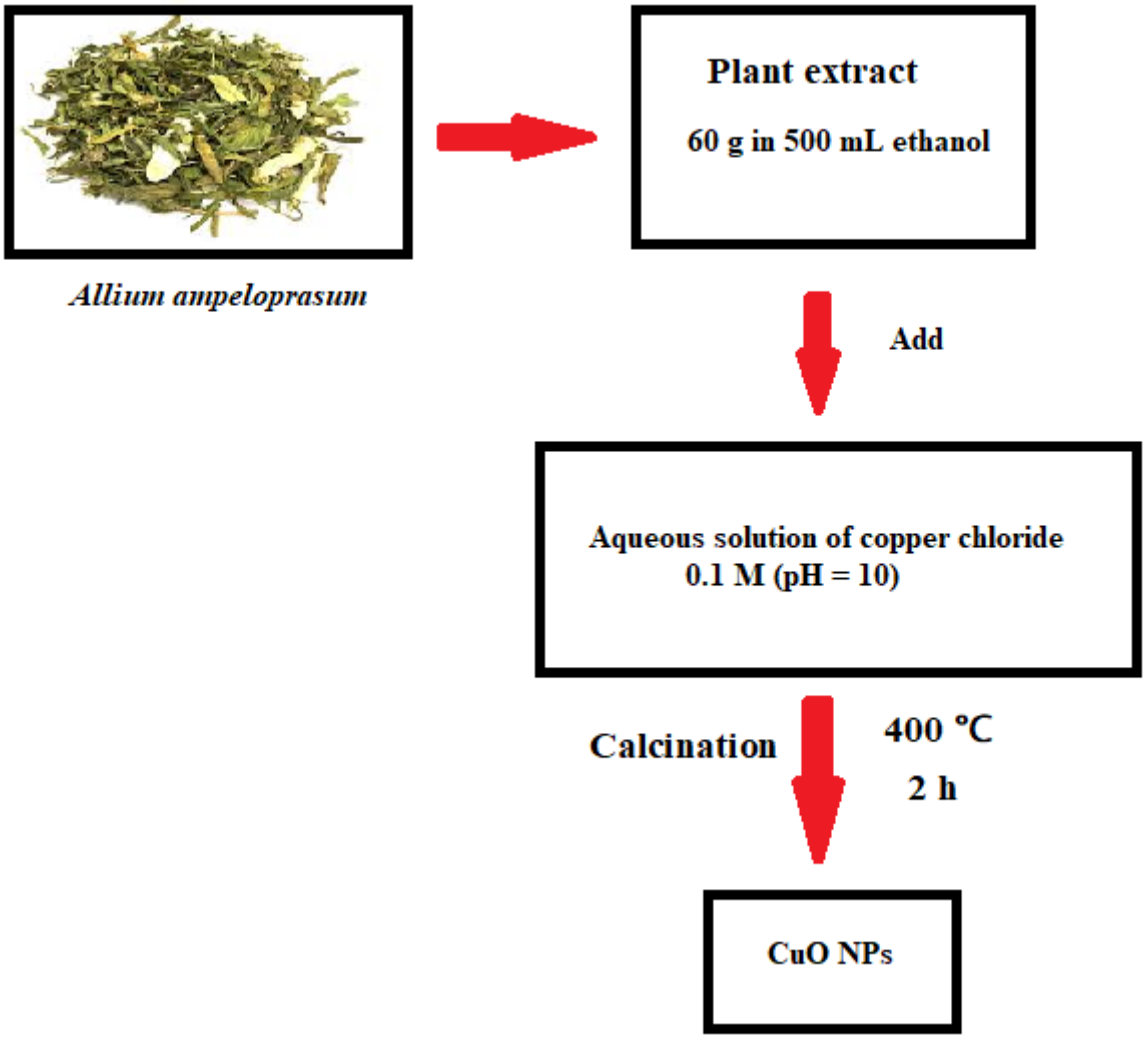

Figure 1

Scheme for plant extract mediated CuO NPs synthesis

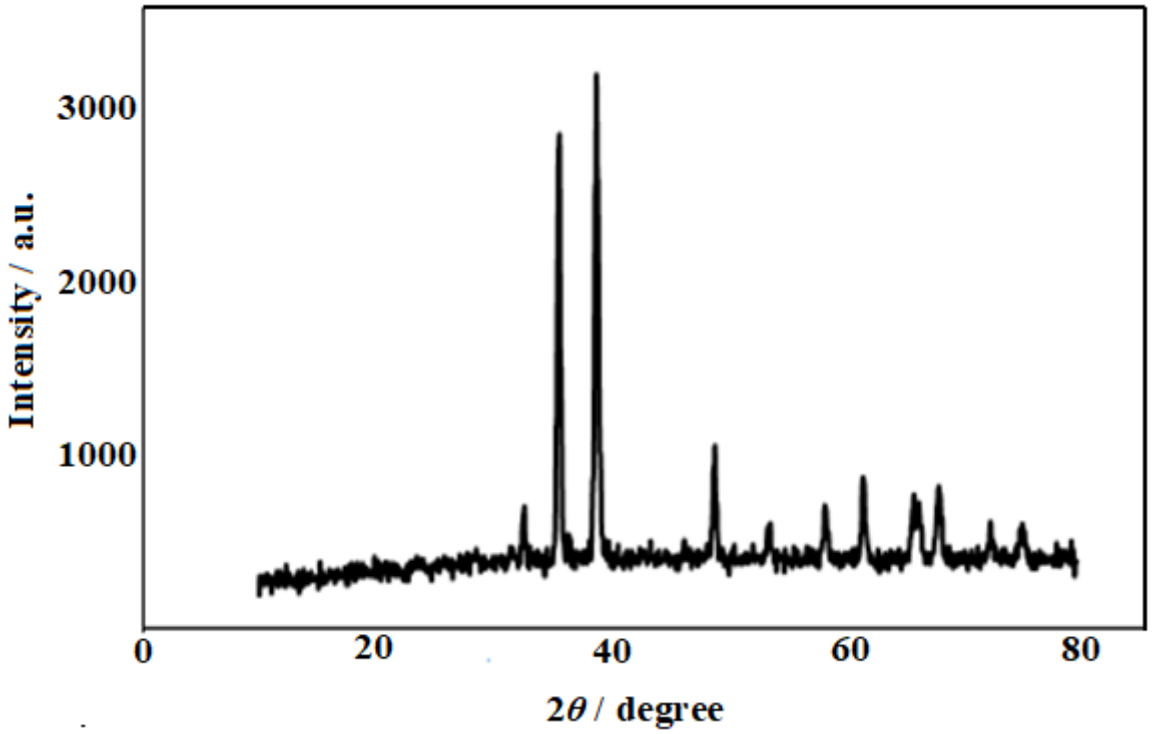

Figure 2

XRD of CuO NPs synthesized with *Allium ampeloprasum* extract

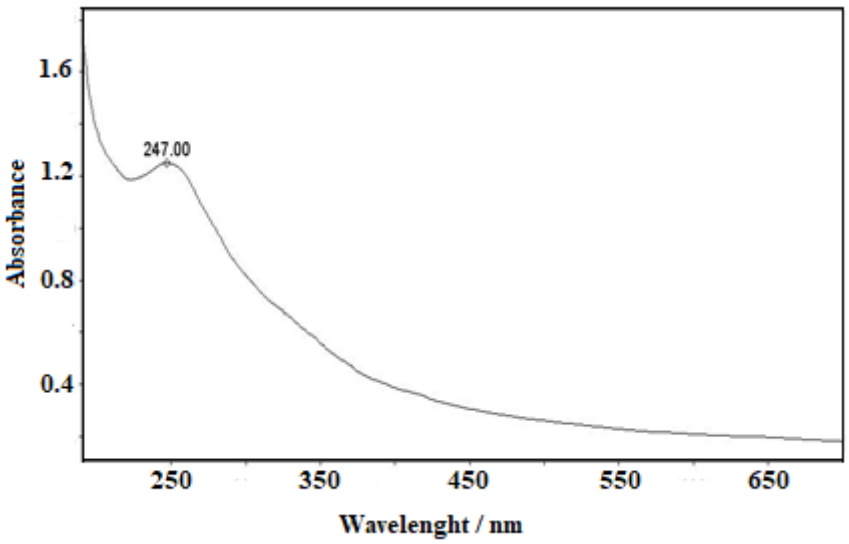

Figure 3

UV-Vis spectra of CuO NPs synthesized with *Allium ampeloprasum* extract

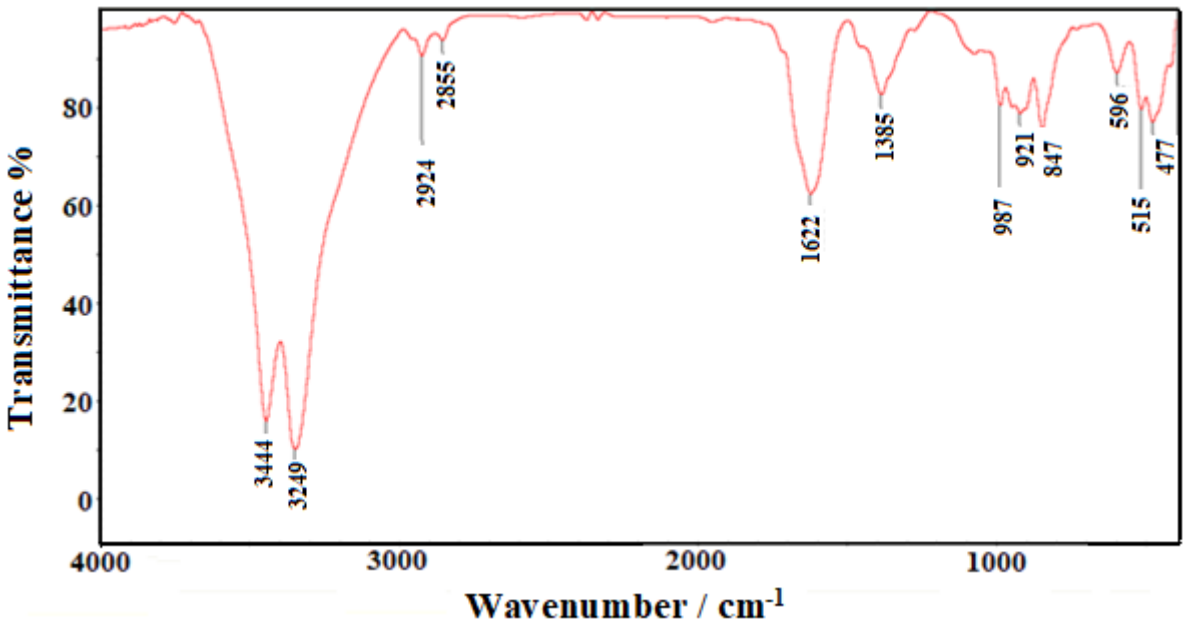

Figure 4

FT-IR spectra of CuO NPs synthesized using *Allium ampeloprasum* extract

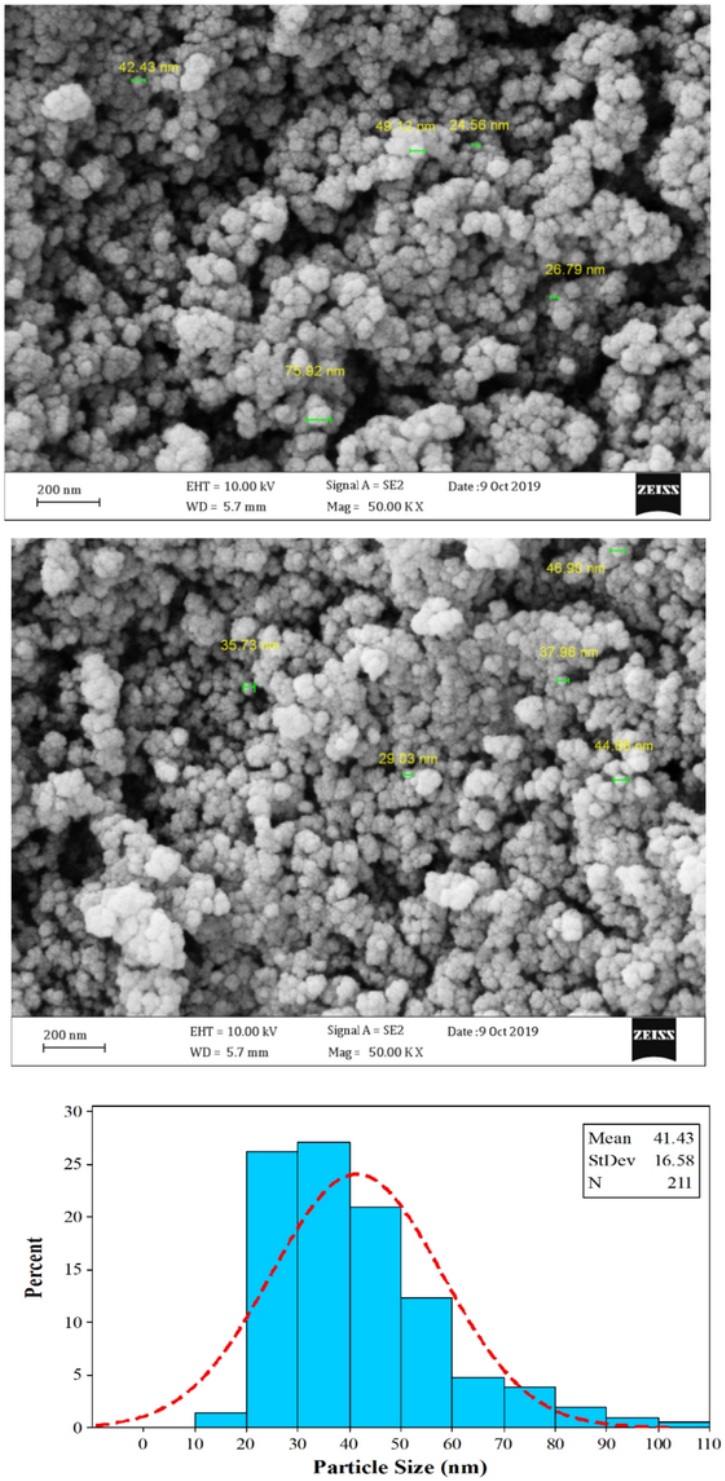

Figure 5

SEM images of CuO NPs synthesized with *Allium ampeloprasum* extract

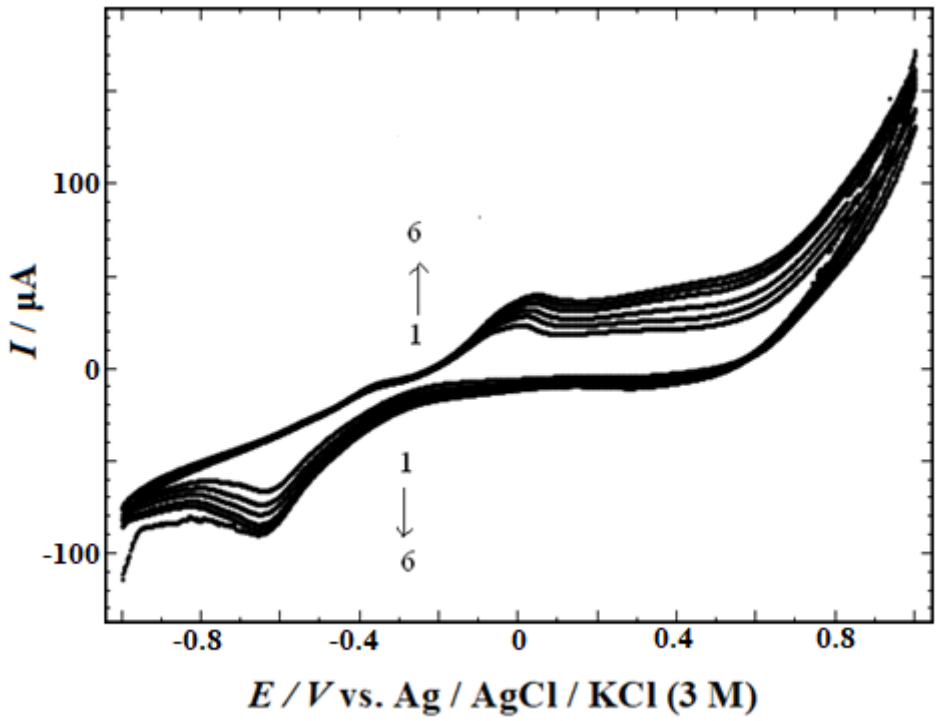

Figure 6

Cyclic polarization behavior of CPE/CuO NPs in 0.1 mol L^{-1} NaOH solution, v=50 mV s^{-1} (6 cycles).

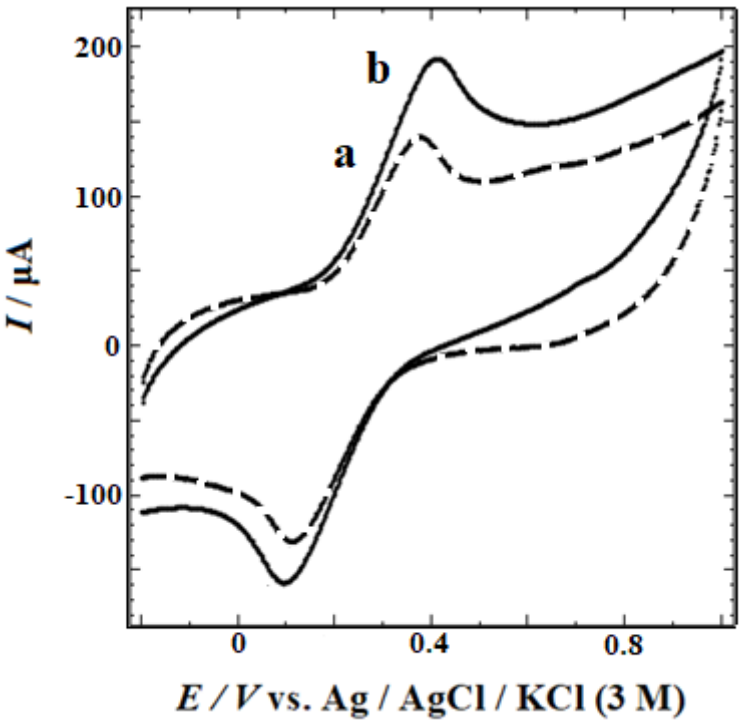

Figure 7

Cyclic voltammograms of a CPE and b CPE/CuO NPs in the presence of 1 mmol L^{-1} $K_4Fe(CN)_6$ solution at a scan rate of 50 mV s^{-1} and in 0.1 mol L^{-1} KCl solution (pH=7.0)

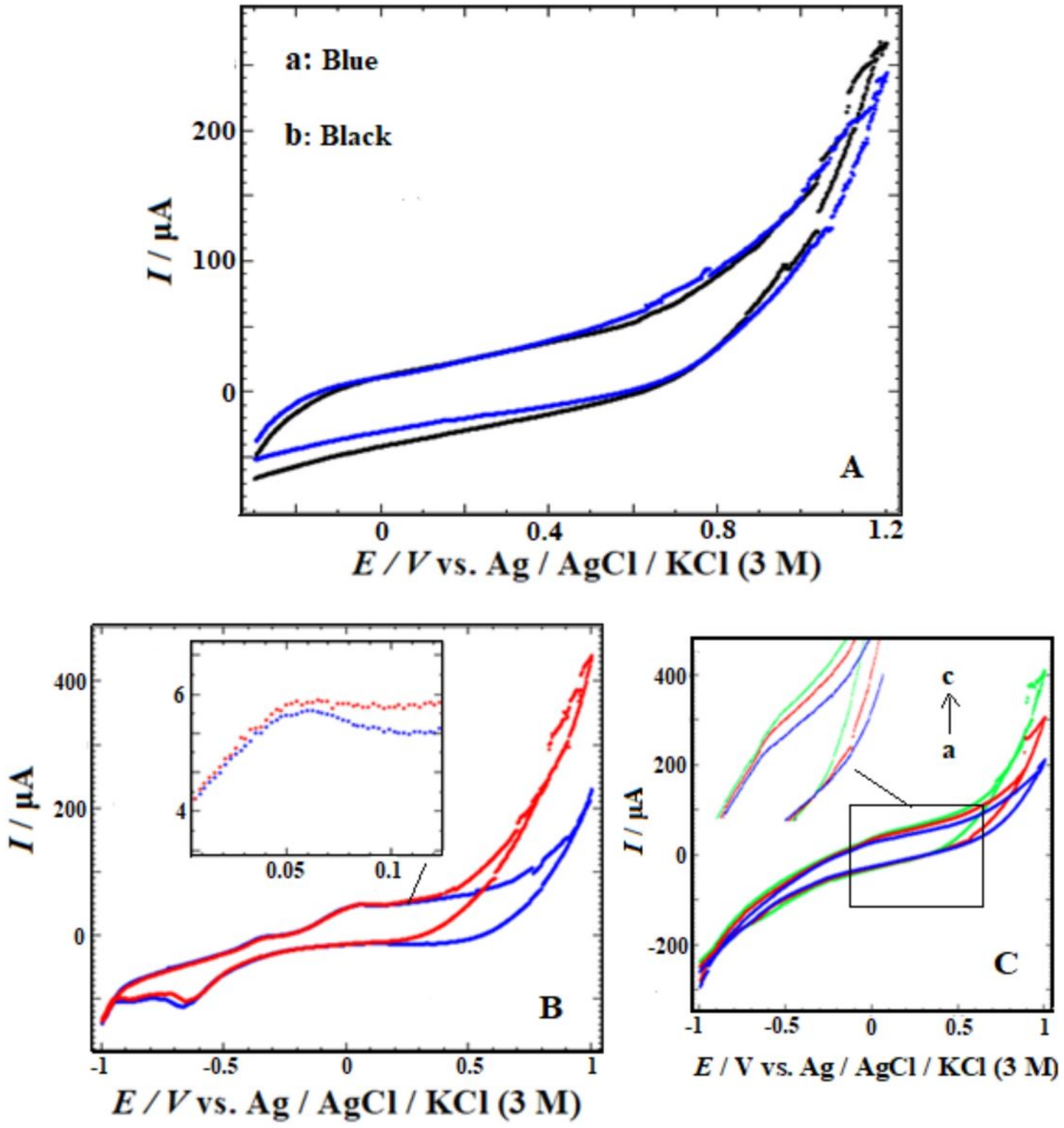

Figure 8

A Cyclic voltammograms of CPE in the absence (a) and presence of 10 µmol L^{-1} glucose (b), **B** as same as (A) but CPE/CuO NPs and (C) Cyclic voltammograms of CPE/CuO NPs in 0.1 mol L^{-1} and the presence of different concentrations of glucose: (a) 20, (b) 40 and (c) 60 µmol L^{-1}, v=20 mV s^{-1}.

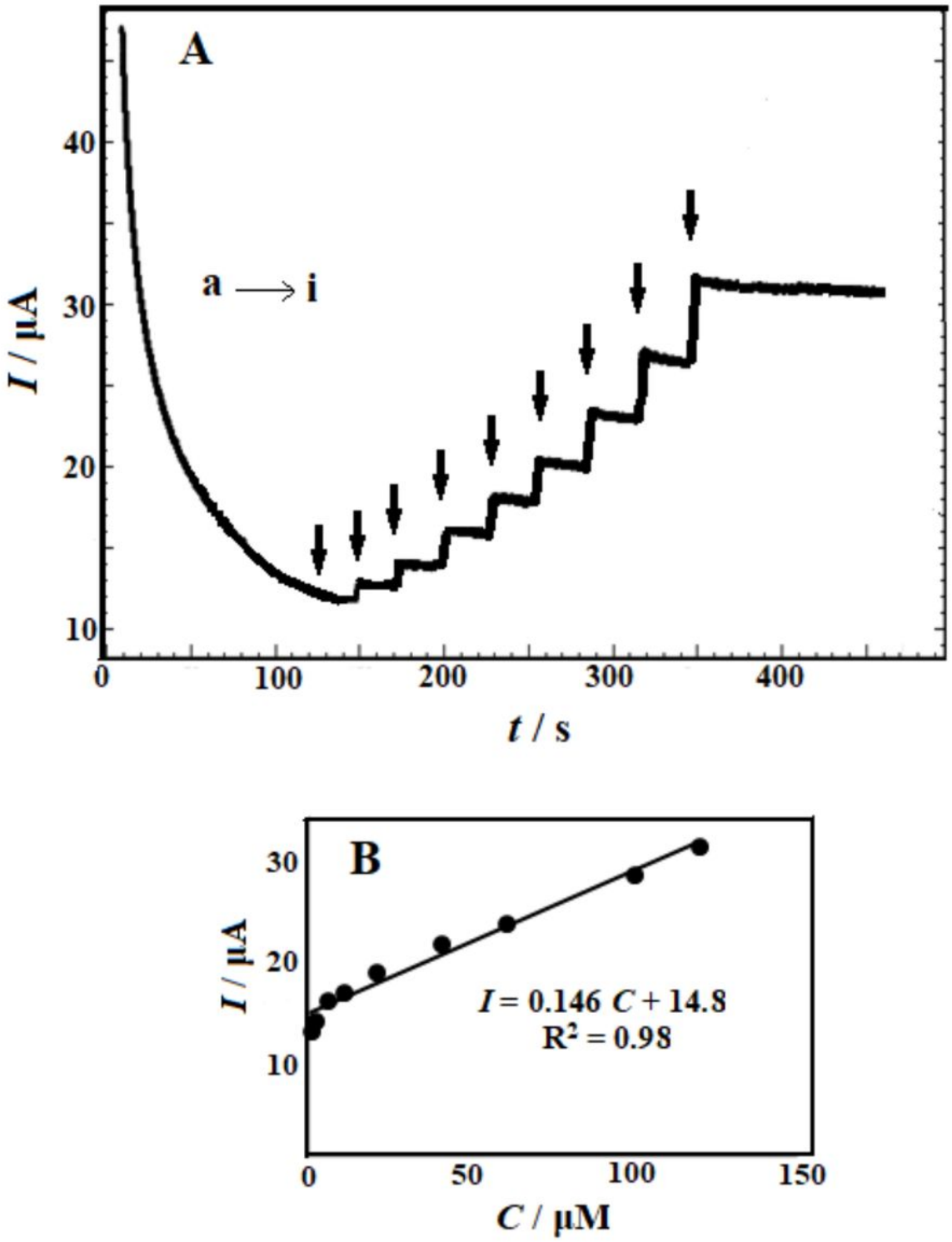

Figure 9

Amperometric responses of CPE/CuO NPs in 0.1 mol L^{-1} NaOH with different concentrations of glucose: a 0, b 1, c 5, d 10, e 20, f 40, g 60, h 100, and i 120 μmol L^{-1}; b corresponding calibration curve (applied potential, 0.1 V)

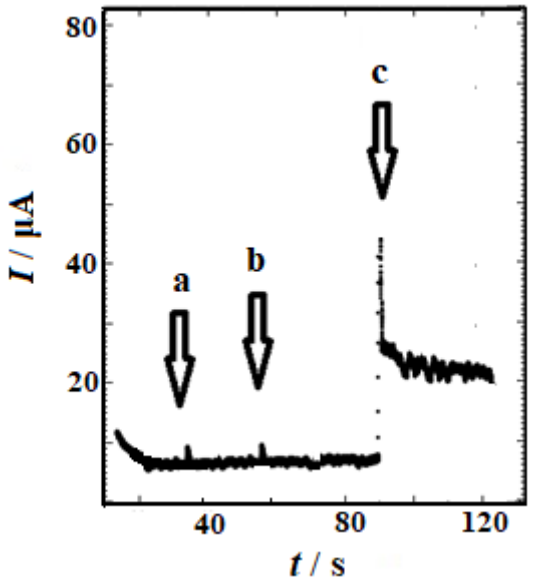

Figure 10

Amperometric responses of CPE/CuO NPs in 0.1 mol L^{-1} NaOH in the presence of 0.1 mmol L^{-1} glucose (c) in the presence of the same concentration of AA (a) and UA (b), applied potential: 0.1 V.